THE 4TH INTERNATIONAL TOPICAL MEETING ON
NUCLEAR THERMAL HYDRAULICS, OPERATIONS AND SAFETY
April 6-8, 1994, Taipei, Taiwan

HEAT TRANSFER CHARACTERISTICS OF ALKALI METALS FLOWING ACROSS TUBE BANKS

K.Sugiyama, R.Ishiguro, Y.Kojima and H.Kanaoka
Department of Nuclear Engineering, Hokkaido University
North13 West8 Sapporo 060, JAPAN
Fax:(81)-11-717-4745

ABSTRACT

For the purpose of getting heat transfer coefficients of alkali metals flowing across tube banks at an acceptable level, we propose to use an inviscid-irrotational flow model, which is based on our flow visualization experiment. We show that the heat transfer coefficients obtained for the condition where only the test rod is heated in tube banks considerably differ from those obtained for the condition where all the rods are heated, because of interference between thick thermal boundary layers of alkali metals. We also confirm that the analytical values obtained by this flow model are in a reasonable agreement with experimental values.

INTRODUCTION

Large computer codes are used for the evaluation of heat transfer performance of intermediate heat exchangers (IHX) and steam generators (SG) in fast breeder reactors (FBR). However, the heat transfer coefficient data to be fed into the codes are not always correctly determined. Experiments on liquid sodium to obtain data necessary for the evaluation of such heat transfer performance require considerable money and time, and the obtained data often do not satisfy the accuracy requirements. Thus, if an analytical method which gives sufficiently accurate heat transfer coefficients is established, it will be very useful to offer data necessary for computer codes at a lower cost and higher efficiency than do experiments.

Since systems of coolant flowing across tube banks, which this paper deals with, are widely used as heat exchangers, heat transfer coefficients of ordinary fluids flowing across tube banks have been extensively studied up to now. However it is difficult to estimate the heat transfer coefficients of alkali metals from those of ordinary fluids accumulated, because of the difference between thermal properties of alkali metals and those of ordinary fluids.

Liquid sodium is a fluid of low Plandtl number, so its heat transfer rate via eddy diffusion is relatively low compared with the heat transfer rate through heat conduction up to a high Reynolds number region. In addition, liquid sodium has a relatively thick thermal boundary layer. Therefore, there is a possibility that a simple inviscid, irrotational flow model neglecting the velocity boundary layer provides a practically accurate estimation of heat transfer coefficients, while no prediction methods on heat transfer coefficients of ordinary fluids have been established because of the turbulent flow field.

There exists no recent study on this type of flow from this view point, as far as we can survey. However, there have been a few analytical studies on heat transfer of liquid metal flowing across tube banks which were published about three decades ago. The papers treated with the system where only one tube of the interior of tube banks is heated (this type of tube banks is referred to as "single-tube(or rod)-heating system" hereafter).

Cess and Grosh determined a flow field using the conducting sheet analogy and theoretically calculated the average Nusselt number.[1] Hsu theoretically determined the average Nusselt number by assuming a cosine-type distribution of hydrodynamic potential.[2] Cess and Grosh compared their analytical result with the experimental data of Hoe et al. who used mercury as the liquid metal.[3] Hsu compared his results with the data of Hoe et al. and Rickard et al. who also used mercury.[4]

These comparisons fairly agreed with each other. Thus, we can expect this type of analysis is useful for practical applications. However, they did not analyze the heat transfer characteristics in tube banks where all tubes are heated.

In actual heat exchangers, all tubes are heated (or cooled). If an alkali metal, a low Prandtl number fluid, is used as the heat transfer medium, the thick thermal boundary layers on adjacent heat transfer tubes strongly interfere with each other. The phenomenon suggests that

the heat transfer characteristics of single-tube-heating systems significantly differ from those of banks where all tubes are heated (the latter system is referred to as "all-tubes(or rods)-heating system" hereafter). Consequently, the heat transfer characteristics of all-tubes-heating systems cannot be predicted from the studies of single-tube-heating system and must be investigated separately.

In our previous study, we numerically determined the heat transfer characteristics of both single-tube-heating and all-tubes-heating systems using an inviscid, irrotational flow model.[5] The obtained values were compared with available experimental data of alkali metals flowing across rod banks, and the validity on the model to estimate heat transfer coefficients was reviewed. As a result, it was confirmed that the analytical values are in a reasonable agreement with experimental data, except for those obtained at the first row in rod banks, regardless of single-rod-heating system or all-rods-heating system. In other words, we could not predict heat transfer coefficients at the first row by using the flow model and it seemed there are limitations of the model. The cause of the disagreement between the experimental value and the analytical value at first row was not explained.

In the present study, at first we carry out a flow visualization experiment by using water flowing across tube banks for the purpose to observe the flow pattern around each tube. From the observation, we clarify the reason of disagreement at first row, and agreement at other rows between the experimental values and the analytical values. We analyse again heat transfer coefficients of alkali metals flowing across rod banks by using an improved inviscid-irrotational model which takes the experimental fact into account. The obtained values are compared with the experimental data, and the validity of the present model is reviewed.

EXPERIMENT FOR FLOW VISUALIZATION

Figure 1 shows a schematic diagram of experimental apparatus for flow visualization, which consists of a tank, a pump and a test section. The tank is a cylindrical container with its volume of about 215 litres. The pump is a centrifugal pump with a flow rate of about 100 l/min in the test section. The test section consists of a calming section and a visualizing section. A set of meshes, made of stainless steel, is mounted in the calming section to make a uniform flow at the inlet of the visualizing section. The visualizing section is a flow channel with a length of 375 mm and a cross section of 150 mm × 80 mm and is made of acrylic plates. The tube banks also consist of acrylic tubes of 30 mm in outer diameter. The visualization was made for banks of staggered tubes with the ratios of pitch to diameter, P/d, of 1.33 and

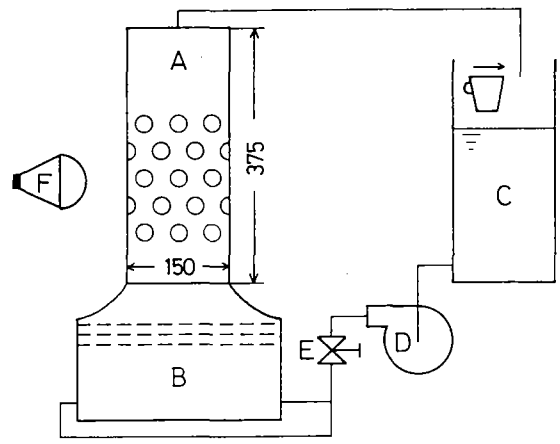

A. VISUALIZING SECTION
B. CALMING SECTION
C. RESERVER TANK
D. CENTRIFUGAL PUMP
E. CONTROL VALVE
F. HALOGEN LAMP

Fig.1 Schematic diagram of experimental apparatus.

1.75.

To visualize flow pattern, alminium powder was used as a tracer, which was poured into water through the tank, and light of a halogen lamp (500W in power) was penetrated through the side walls of the visualizing section horizontally. When photographing, the aperture of camera was kept approximately constant and the exposing time was adjusted appropriately to the flow velocity.

We determined the average flow velocity at minimum flow path of tube banks by measuring the flow rates of circulating water returned to the inlet of tank. So Reynolds number, Re_{max}, used here is based on the average flow velocity at the cross section of the minimum flow path. The experiment for visualization was carried out in a range of $1750<Re_{max}<8870$.

EXPERIMENTAL RESULTS

Photos 1 and 2 show flow patterns of $Re_{max}=8840$ at the first row and the third row in the tube bank of P/d=1.75, respectively. As shown in Photo 1, a steadily closed separation region is always formed at the rear of tube in the first row, and the boundary between the main flow and this region can be seen clearly (the broken line schematically shows the boundary). The flow velocity in this region is much smaller than that of the main flow, so that we can regard this region as the dead water region. However, at the rear of tube in the third row, this closed separation region does not appear as clearly as that in the first row, as shown in Photo 2. The flow behavior in this rear region is very unstable and complicated, and it is obvious that the flow field with a strongly unstable motion will

make an effective heat transfer from the rear surface in a time average, compared with the behavior in the first row. This flow behavior presumably originates in the instability caused by the interference between the main flow, the separation region and upstream tubes. The phenomena observed at the third row appear also at the second row, and on and after the fourth row.

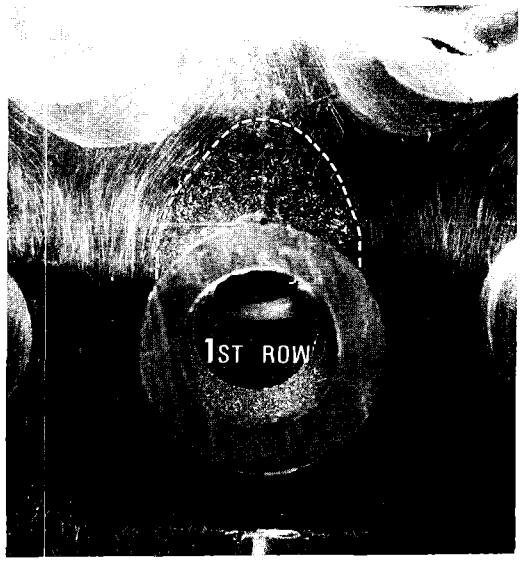

Photo 1 Flow pattern of Re_{max}=8840 at the first row in the tube bank of P/d=1.75.

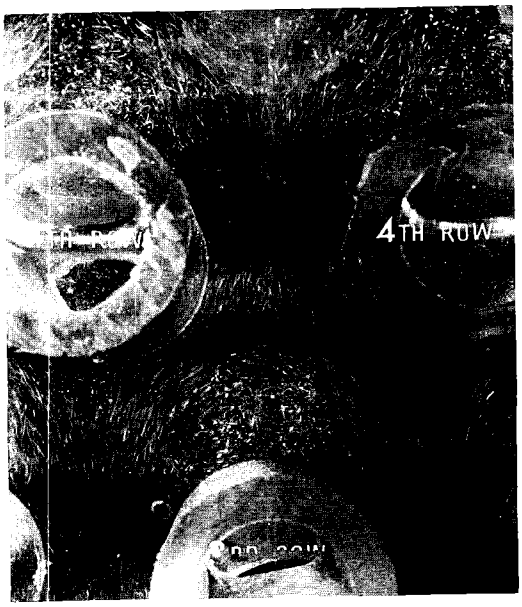

Photo 2 Flow pattern of Re_{max}=8840 at the third row in the tube bank of P/d=1.75.

It is expected from this experimental fact that the heat transfer rates on the tubes set at the first row will be smaller than those at the tubes on and after the second row. This expectation corresponds to the experimental fact of Kalish and Dwyer, in which heat transfer coefficients of the rod is minimum at first row and increases up to fifth row.[7]

Photos 3 and 4 show flow patterns at the first row and the third row in the case of P/d=1.33 for Re_{max}=7540, respectively. Flow pat-

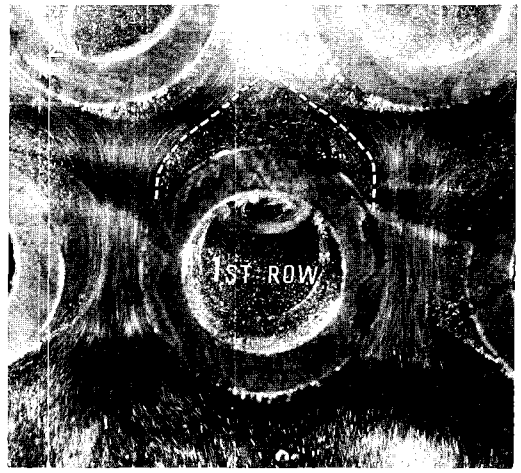

Photo 3 Flow pattern of Re_{max}=7540 at the first row in the tube bank of P/d=1.33.

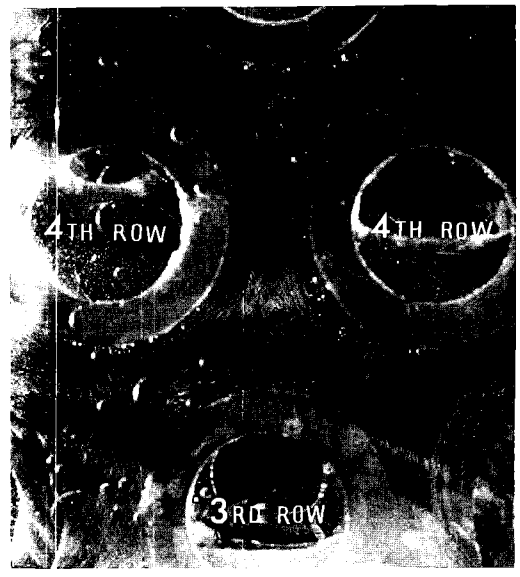

Photo 4 Flow pattern of Re_{max}=7540 at the third row in the tube bank of P/d=1.33.

terns are similar to those in the case of P/d=1.75. A closed separation region clearly appears at the rear of tube in the first row which is distinguished from the main flow by the broken line in Photo 3, and it does not appear evidently at the rear of tube in the third row.

We found the difference between the flow patterns around the tubes at the first row and that around tubes on and after the second row qualitatively. According to this experimental fact, we introduced an inviscid-irrotational flow model with the dead water region at only first row, and used an inviscid-irrotational flow model without the separation region on and after second row.

The visualization experiment was carried out in a range of $1750<Re_{max}<8870$, and the fact similar to that mentioned above was observed in the whole range. This Reynolds number range approximately covers the lower-half range out of $50<Pe_{max}<300$ in an experiment for NaK (Pr=0.017) described later.

BASIC EQUATIONS AND ANALYSIS

The present numerical analysis deals with the bank of staggered heating rods encircled by a chain-dotted line shown in Fig.2. The basic equations of non-dimensional flow field, fluid temperature field, and rod sheath temperature field used in this study are given below:

$$\nabla^2\Psi = 0 , \qquad (1)$$

$$\nabla^2 T_f = \frac{Pe}{2}\frac{dT_f}{dt} , \qquad (2)$$

$$\nabla^2 T_s = 0 , \qquad (3)$$

where $\nabla^2=\partial^2/\partial X^2 + \partial^2/\partial Y^2$, $d/dt=\partial\Psi/\partial Y\cdot\partial/\partial X-\partial\Psi/\partial X\cdot\partial/\partial Y$ in the Cartesian coordinates, and $\nabla^2=\partial^2/\partial\xi^2 + \partial^2/\partial\eta^2$, $d/dt=\partial\Psi/\partial\eta\cdot\partial/\partial\xi-\partial\Psi/\partial\xi\cdot\partial/\partial\eta$ in a cylindrical (η,ξ) coordinates.

Since Equation (1), the flow field equation, assumes an inviscid, irrotational flow and neglects viscous terms (i.e., no eddy flow), it takes the form of the Laplace equation. Equation (2) is the energy equation for incompressible fluids. Equation (3) is the heat conduction equation relating to sheath, which is introduced to match the boundary conditions of analysis with those of experiment.

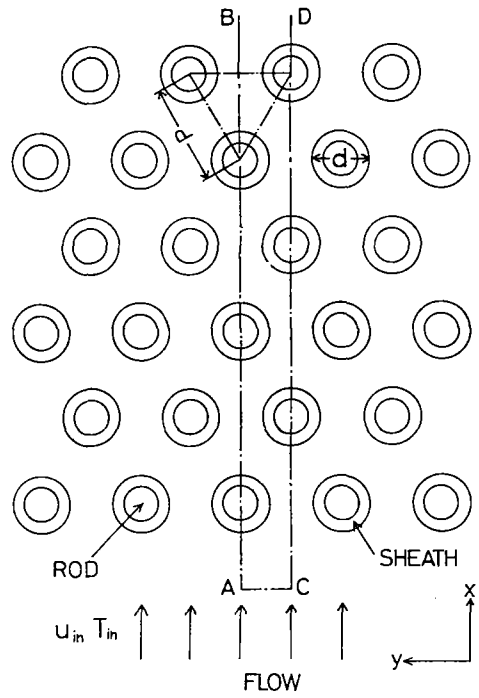

Fig.2 Cross sectional view of staggered rods.

Experiments on alkali metals often use copper as a sheath material to allow accurate measurements of the surface temperature of heating rods. In these cases, a peripheral heat flow occurs through the sheath, thereby dissatisfying the boundary conditions of uniform heat flux on the sheath surface. Heat generating rods of this type include Nichrome coil (or tube) heating elements in an axially symmetrical arrangement, which leads to uniform heat flux at inside surface of the sheath. To match the boundary conditions of analysis with those of experiments, the boundary condition of uniform heat flux at

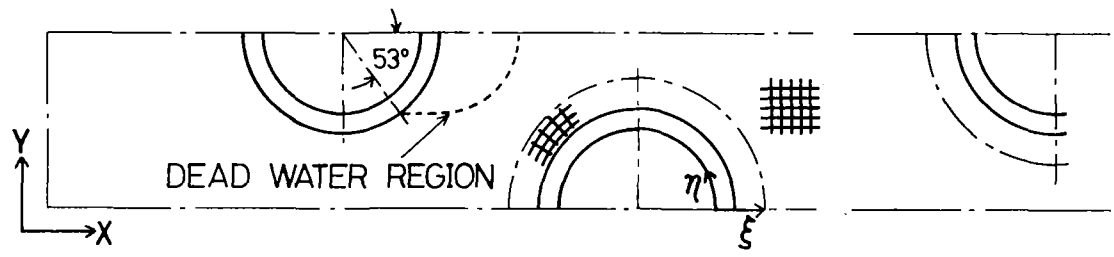

Fig.3 Coordinate system and shape of the dead water region for numerical analysis

inside surface of the sheath is given to the analysis.

In Fig.2, the boundary conditions at line AC are uniform velocity and uniform temperature, and the symmetric boundary conditions are given at lines AB and CD. The location of BD is far downstream, and the boundary conditions for BD are given with an assumption that gradients of fields along the flow direction are "zero". The present numerical analysis is carried out by using a cylindrical coordinates (ξ,η coordinates) in the vicinity of rods and the Cartesian coordinates for other areas as shown in Fig.3. Therefore the boundary conditions are written as follows:

$$
\left.
\begin{aligned}
&\xi=\xi_1 : \frac{\partial T_s}{\partial \xi} = -\pi \frac{\lambda_f}{\lambda_s} , \\
&\xi=\xi_0 : T_f = T_s , \frac{\partial T_f}{\partial \xi} = \frac{\partial T_s}{\partial \xi} \frac{\lambda_s}{\lambda_f} , \\
&\qquad \Psi = 0 \quad \text{or} \quad \Psi = P-1 , \\
&Y=0 , \ \eta=0,1 : \\
&\qquad \frac{\partial T_f}{\partial Y} = 0 , \frac{\partial T_f}{\partial \eta} = 0 , \\
&Y=P , \ \eta=0,1 : \\
&\qquad \frac{\partial T_s}{\partial \eta} = 0 , \Psi = 0 , \\
&\qquad \frac{\partial T_f}{\partial Y} = 0 , \frac{\partial T_f}{\partial \eta} = 0 , \\
&\qquad \frac{\partial T_s}{\partial \eta} = 0 , \Psi = P-1 , \\
&X=X_{in} : T_f = 0 , \Psi = \frac{P-1}{P} Y , \\
&X=X_{max} , \ \eta=0.5 : \\
&\qquad \frac{\partial T_f}{\partial X} = 0 , \frac{\partial T_f}{\partial \eta} = 0 , \\
&\qquad \frac{\partial T_s}{\partial \eta} = 0 , \frac{\partial U}{\partial X} = 0 , \frac{\partial U}{\partial \eta} = 0 .
\end{aligned}
\right\} \quad (4)
$$

The finite difference equations are obtained by applying the central difference approximation to the diffusion terms in each basic equation and by applying an upwind difference with third-order accuracy developed by Kawamura and Kuwahara to the convection terms.[6] The dimensionless lattice spacings are taken as $\Delta X=\Delta Y=0.025$, $\Delta\xi=\Delta\eta=0.025$ based on a preliminary calculation. The lattice point values on the junction of each coordinate system are determined by the interpolation of the lattice point values of the other coordinate system. The convergence is judged from heat balance in the system and the values of Nusselt number.

According to the experimental fact observed by visualization, we model the closed separation region as the dead water region at only the rear of rod set in the first row in the present numerical analysis. The area and geometrical shape of this dead water region, which is shown in Fig.3, fairly corresponds to those shown in Photo 1. We regard it as a dead water region, that is, the flow velocity is simply zero in the region. Thus, we must add a following boundary condition, which is applied at the dead water region, to Equations (4) :

$$U = V = 0 \qquad (5)$$

As a result, we assume that heat is transferred by only conduction in the region, and therefore solve only heat conduction equation.

ANALYTICAL RESULTS AND DISCUSSION

Kalish and Dwyer carried out heat transfer measurement using a system of NaK (Pr=0.017) flowing across a bank of staggered rods, which had a P/d value of 1.75 and 9 rows in the flow direction with a total of 63 rods.[7] They obtained data both for single-rod-heating system and for all-rods-heating system.

For the single-rod-heating system, Fig.4 shows the comparison among average Nusselt numbers of present analysis, those of laminar flow analysis and the experimental data of Kalish and Dwyer. These comparisons are made at the first, second, and fifth rows of the rod banks. The Nusselt numbers of those cases are evaluated at the inlet temperature. The experimental values increase as the row numbers increase, which is probably due to the fact that eddy heat diffusion increases further downstream owing to the turbulent effect caused by upstream rods. The result of the previous analysis depended very little on the number of the rows. As a result, the analysis gave a value approximately 30% higher than the experimental value at the first row.

The result of present analysis in the single-rod-heating system gives an about 10% lower value than the experimental value at the first row, where we take account of the dead water region in the rear of rod. This result reflects the fact that heat is not transferred by convection but only transferred by conduction. The reason that the present analytical value is a little smaller than the experimental value is probably that the flow velocity in that region is not strictly zero in the real field. However, so far as this analysis underestimates heat transfer coefficients with this degree of error between experimental value and analytical value, it will be useful in practical use.

We observed the flow field in the low half of Peclet number range in Kalish and Dwyer's experiment. From the comparison between the experimental result and the present value in the first row shown in Fig.4, we can easily confirm that the dead water model as a first-order approximation is reasonable in the whole range up to Pe_{max}=300. We must also mention here the

present analytical result is somewhat higher than that obtained in the laminar flow field in the whole range compared. For the second row and the fifth row, the average Nusselt numbers of the present analysis are approximately equal to and about 10% lower than those of the experimental result, respectively.

Figure 5 shows a comparison of average Nusselt numbers in all-rods-heating system, which is important for practical use. In this case, Nusselt numbers are evaluated by the bulk temperature at the cross-section of the minimum flow path. Experimental values in this system increase further downstream similar to the trend seen in the single-rod-heating system, and the previous result showed an approximately 40% higher value than the experimental value at the first row.

The result of present analysis on the first row in the all-rods-heating system, where we take account of the dead water region in the rear of rod, shows an approximately 30% lower value than the previous analytical value. Thus, the result shows an approximately 15% higher value than the experimental value at a low Peclet number, and shows an approximately 8% lower value than the experimental value at a high Peclet number. Similar to the case of the single-rod-heating system, this analytical value is smaller than the previous analytical value because of the fact that heat is transferred only conduction in this analysis. On the third row, the analytical value at a low Peclet number is approximately 20% higher than the experimental value, but the calculated value at a high Peclet number is almost equal to the experimental value. In the fifth row, the analytical value is approximately 10% lower than the experimental value at the high Peclet number, but is approximately 10% higher than the experimental value at a low Peclet

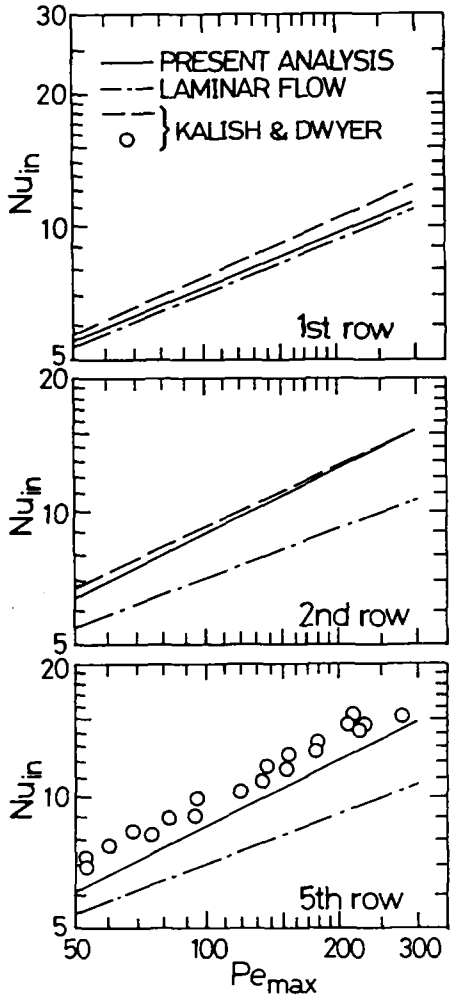

Fig.4 Comparison between the present values and experimental results for NaK flow with only test rod heated.

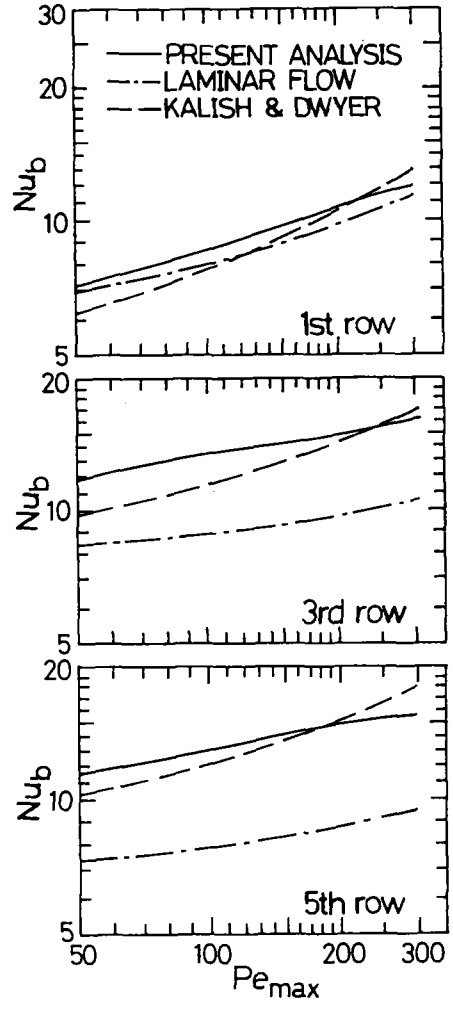

Fig.5 Comparison between the present values and experimental results for NaK flow with all rods heated.

number.

As mentioned in the previous paper, in the experiment performed with the all-rods-heating system, the evaluation of bulk temperature is difficult, which may result in an experimental error. Actually, at the first row of a low Peclet number region, this experimental value of Kalish and Dwyer is smaller than the value obtained by the numerical analysis in the laminar flow field which we calculated once. We can not physically expect to get Nusselt numbers lower than the values obtained in the laminar flow field. Nevertheless, the difference with solution of laminar flow remains rather small for the data obtained from a rod banks in NaK flow, in which accurate measurement is difficult, and we judge that the magnitude of error is not recognized as a problem on the comparison in Fig.5, at least for the present. Therefore, we may conclude this analytical values in all-rods-heating system are in a reasonable agreement with the experimental value.

CONCLUSION

We observed the behavior of fluid flowing across tube banks by the flow visualization experiment with water. The experiment showed that the closed separation region is evidently formed at the rear of the tubes (rods) at the first row in tube banks and does not appear clearly at the rear of the tubes on and after second row. According to this experimental fact, we introduced an inviscid-irrotational flow model with the dead water region at only first row, and used an inviscid-irrotational flow model without the separation region on and after second row for the purpose to estimate the heat transfer coefficients of alkali metals flowing across rod banks.

As a result, we could show that the obtained analytical values are in a reasonable agreement with experimental values regardless of single-rod-heating system or all-rods-heating system and an estimation of heat transfer characteristics of alkali metals is possible at a generally acceptable level by the present analysis.

Acknowledgement : The authors wish to acknowledge the financial support for the present research by the Tanigawa Foundation.

NOMENCLATURE

d:	rod diameter
Nu:	average Nusselt number
P:	pitch
Pe:	Peclet number
r:	radial distance
Re:	Reynolds number
T:	temperature
u:	velocity in x direction
U,V:	dimensionless velocity in X,Y direction
x,y:	Cartesian coordinates
X,Y:	dimensionless Cartesian coordinates
η:	θ/π
θ:	angle
ξ:	$(1/\pi)\ln(r/r_o)$
Ψ:	dimensionless stream function

Subscripts

b:	value based on bulk temperature
ex:	exit
f:	fluid
i:	inner surface of sheath
in:	inlet or value based on inlet temperature
max:	value based on the maximum velocity at minimum flow area
o:	outer surface of sheath
s:	sheath

REFERENCES

1. R.D.CESS and R.J.GROSH,"Heat transmission to Fluids With Low Prandtl Numbers for Flow Through Tube banks," *Trans. ASME 80*, 677 (1958).

2. C.J.HSU,"Analytical Study of Heat Transfer to Liquid Metals in Cross-Flow Through Rod Bundles," *Int. J. Heat Mass Transf. 7*, 431 (1964)

3. R.J.HOE, D.DROPKIN and O.E.DWYER,"Heat-Transfer Rates to Crossflowing Mercury in a Staggered Tube Bank-I," *Trans. ASME 79*, 899 (1957).

4. C.L.RICKARD, O.E.DWYER and D.DROPKIN,"Heat-Transfer Rates to Cross-Flowing Mercury in a Staggered Tube Bank-II," *Trans. ASME 80*, 646 (1958).

5. K.SUGIYAMA, R.ISHIGURO and F.IMAEDA,"A Numerical Study of Heat Transfer to Alkali Metals Flowing Across Rod Banks," *Proc. the 1st JSME/ASME Joint Int. Conf. on Nuclear Eng.*, 515 (1991).

6. T.KAWAMURA and K.KUWAHARA,"Computation of High Reynolds Number Flow around a Circular Cylinder with Surface Roughness," *AIAA-84-0340*, AIAA (1984).

7. S.KALISH and O.E.DWYER,"Heat Transfer to NaK Flowing Through Unbaffled Rod Bundles," *Int. J. Heat Mass Transf. 10*, 1533 (1967).

Session 24
Severe Accident Management-I